Progress In Electromagnetics Research M, Vol. 31, 263–278, 2013

SIMULATION OF SAR UNDER ULTRA-WIDE BAND ELECTROMAGNETIC PULSE IN HUMAN TISSUE

Teng Jiao, Xiao Yu, Hao Lv, Yang Zhang, Hui Jun Xue, Yan Wang, and Jian Qi Wang* †

College of Biomedical Engineering, The Fourth Military Medical University, Xi'an 710032, China

Abstract—In this study, a three-dimensional (3-D) structural model of an adult male body, including 12 kinds of tissues and organs, was analyzed using a 3-D model design application (i.e., 3ds Max). The standard model of Asians was used as reference. The electrical parameters of brain tissues at different electromagnetic frequencies were introduced to obtain the electromagnetic model. Computational electromagnetic software based on the finite-difference time-domain was used to calculate the model absorption of electromagnetic waves under ultra-wide band electromagnetic irradiation. The specific absorption rates (SARs) of the ensemble average and the model human tissue were also obtained. This study aims to provide a parameter for the development of electromagnetic radiation protection standards, and to discuss related research.

1. INTRODUCTION.

Since the development of electronic technology in the 1980s, semiconductor devices and integrated circuits have been increasingly applied to many devices. However, electromagnetic pulses pose destructive and hazardous effects on modern instruments. Such effects cannot be underestimated. Thus, extensive studies have been conducted internationally to investigate the possible biological effects of low-power electromagnetic irradiation and of continuous wave in organisms and its dosimetry. Furthermore, significant advancements have been achieved in the studies on the endocrine, digestive, reproductive, nervous, and cardiovascular systems as well

Received 20 May 2013, Accepted 22 June 2013, Scheduled 9 July 2013

* Corresponding author: Jian Qi Wang (WangJq@fmmu.edu.cn).

† The first three authors contributed equally to this work and should be regarded as co-first authors.

as on the carcinogenic properties of electromagnetic waves. With the development of ultra-wide band (UWB) in recent years, studies on the biological effects of UWB electromagnetic pulses have emerged. For example, previous works explore the biological effects under UWB irradiation [1–3]. One study discusses the latest progress in the research on the biological effect mechanism of UWB electromagnetic pulses [4]. An electromagnetic pulse has a greater destructive effect on biological cells than continuous waves. Thus, the failure mechanism of electromagnetic pulses should be explored further. However, the effect of UWB electromagnetic pulses on organisms and its possible value have been investigated in biomedical research only recently. In the present study, a computational electromagnetic application based on finite-difference time-domain (FDTD) is used to calculate the model absorption of electromagnetic waves under UWB electromagnetic irradiation. The specific absorption rates (SARs) of the ensemble average and the model human tissue are also obtained.

2. BASIC PRINCIPLES OF THE CALCULATION OF ELECTROMAGNETIC WAVE SAR

A general solution method for Maxwell's equations, which describe the evolution of electromagnetic waves in periodical materials, is the FDTD method [5]. Since its introduction 70 years ago, this method has become popular because of certain advantages: (a) simplicity of explicit numerical scheme, (b) applicability to different geometries (only grids should be adapted), and (c) explicit description of the properties of non-linear materials [6].

The most commonly used electromagnetic dosimetry in complex biological models is the FDTD, which is a numerical method based on the difference principle. The FDTD transforms the electromagnetic continuous domain into a discrete system, i.e., the FDTD uses arithmetic solutions on each discrete point to infinitely approach the real solution in the continuous field. The FDTD is an approximate calculation method and translates Maxwell's curl equation into a simple and comprehensible differential equation, with Yee cell as the electromagnetic field discrete unit of space. With computer technology, the FDTD can process complex electromagnetic issues [7–11].

In this study, induced electric fields were generated in organisms under the influence of external electromagnetic fields. The size of the induced electric field is related to electromagnetic frequency, intensity, direction, etc. Moreover, the shape, size, and electrical parameters of tissue as well as the relative position between the radiation source and irradiated object and the nearby objects are also related to size. SAR was extensively applied in the electromagnetic dosimetry to measure the induced electric field generated from electromagnetic radiation in living tissue and to evaluate the effect of different electromagnetic waves on different organisms at different positions. The international unit of SAR is W/kg, which indicates something to the effect of the time derivative of the mass absorption or electromagnetic wave energy consumption of a biological target tissue per unit.

When the incident field is a time-harmonic field, the aforementioned equation can be expressed as

$$SAR(i,j,k) = \frac{\sigma(i,j,k)}{2\rho(i,j,k)}|E_{\max}|^2 \tag{1}$$

where (i, j, k) indicates a node in the discretized model grid, σ is the living tissue conductivity (S/m), ρ is the mass density (kg/m^3) of the living tissue, and $|E_{\max}|$ is the electric field amplitude of the node.

Maxwell's curl equation is

$$\nabla \times H = \frac{\partial D}{\partial t} + J \tag{2}$$

$$\nabla \times E = -\frac{\partial B}{\partial t} - J_m \tag{3}$$

where E is the electric field strength (N/C), D the electric flux density (C/m^2), H the magnetic field strength (A/m), B the magnetic flux density (Wb/m^2), J the current density (A/m^2), and J_m the magnetic current density (V/m^2). As $D = \varepsilon E$, $E = \mu H$, $J = \sigma E$, and $J_m = \sigma_m H$, ε refers to permittivity (F/m), μ is the permeance coefficient (H/m), σ the conductivity (S/m), and σ_m the magnetic permeability (Ω/m).

Let $f\,(x, y, z, t)$ represent a component of E or H in the system of rectangular coordinates:

$$f\,(x,y,z,t) = f\,(i\Delta x, j\Delta y, k\Delta z, n\Delta t) = f^n\,(i,j,k) \tag{4}$$

where Δx, Δy, Δz are the space steps along the x, y, and z directions, respectively, in the rectangular grid. Δt is the time step, and n indicates n grid.

Take the first-order partial derivative of $f\,(x, y, z, t)$ as the central difference approximation:

$$\left.\frac{\partial f\,(x,y,z,t)}{\partial x}\right|_{x=i\Delta x} \approx \frac{f^n\left(i+\frac{1}{2},j,k\right) - f^n\left(i-\frac{1}{2},j,k\right)}{\Delta x} \tag{5}$$

$$\left.\frac{\partial f\,(x,y,z,t)}{\partial y}\right|_{y=j\Delta y} \approx \frac{f^n\left(i,j+\frac{1}{2},k\right) - f^n\left(i,j-\frac{1}{2},k\right)}{\Delta y} \tag{6}$$

$$\left.\frac{\partial f(x,y,z,t)}{\partial z}\right|_{z=k\Delta z} \approx \frac{f^n\left(i,j,k+\frac{1}{2}\right)-f^n\left(i,j,k-\frac{1}{2}\right)}{\Delta z} \tag{7}$$

$$\left.\frac{\partial f(x,y,z,t)}{\partial t}\right|_{t=n\Delta t} \approx \frac{f^{n+1/2}(i,j,k)-f^{n-1/2}(i,j,k)}{\Delta t} \tag{8}$$

In practice, Yee cells are cubic; thus, $\Delta x = \Delta y = \Delta z = \delta$ with the same intervals. Eq. (3) can be converted into a differential equation as follows:

$$E_x^{n+1}\left(i+\tfrac{1}{2},j,k\right) = \frac{1-\frac{\sigma(m)\Delta t}{2\varepsilon(m)}}{1+\frac{\sigma(m)\Delta t}{2\varepsilon(m)}} \cdot E_x^n\left(i+\tfrac{1}{2},j,k\right) + \frac{\frac{\Delta t}{\varepsilon_0\delta}}{\varepsilon_r(m)+\frac{\sigma(m)\Delta t}{2\varepsilon_0}}$$
$$\cdot\Big[H_z^{n+1/2}\left(i+\tfrac{1}{2},j+\tfrac{1}{2},k\right)-H_z^{n+1/2}\left(i+\tfrac{1}{2},j-\tfrac{1}{2},k\right)$$
$$-H_y^{n+1/2}\left(i+\tfrac{1}{2},j,k+\tfrac{1}{2}\right)+H_y^{n+1/2}\left(i+1/2,j,k-1/2\right)\Big]$$

As shown in the previous equation, the node and average SAR can be obtained with the induced electric field of any point in the human body. The average SAR of the same media in the human body and the SAR distribution in a profile of the human body can also be obtained.

3. SAR CALCULATION WITH THE FDTD

3.1. Model Establishment of Bio-electromagnetic Dosimetry

In the study of bio-electromagnetic dosimetry, the bio-tissue model with an irregular geometrical shape and nonhomogeneous electric characteristics plays an important role in solving the electromagnetic effect of bio-tissues.

In using the FDTD method to analyze the phenomenon of bio-tissue electromagnetic scattering, the geometry and related physical parameters of the 3-D model must be precisely described. The description can be generated by incorporating the information on size, electric parameters, etc. and then by meshing the model via the FDTD. Generally, the surface of simple objects can be fitted by simple curves and then yield a simple model. However, modeling real objects is complicated.

When constructing a simple 3-D cube model, the target area was irradiated first using electromagnetic waves and then meshed. Finally, the corresponding electric parameters of each cell were imposed according to its position in relation to the target area.

3ds Max is a 3-D design software that can model the complicated biological body, provide friendly user interface, and reduce the complexity of the work. The DXF format is available both in 3-D model design and in the finite element method software. Using 3ds Max, a 3-D human model can be generated in DXF format and then read in 3-D electromagnetic simulation software (e.g., XFDTD, EMPIRE, and FEMLAB). The procedure simplifies the meshing process and the FEM calculation [12].

3.2. Structural Model of an Adult Male Human Body

The difficulties in operating 3ds Max and model size for subsequent FDTD calculation were considered in practical modeling. By calling the 3ds Max model library was accessed to perform human-body modeling, and then; the detailed parts in of the hands of the human model were deleted removed, because of a very small percentage of hands in practical modeling.

Based on the medical human anatomy atlas and on the anatomical and physiology physiological structure of Chinese men and women, particularly in terms of the major tissues or organs, NURBS drawing (surface technology of interactive 3-D simulation curve) in 3ds Max was used to draw the 3-D model of an adult male human with a height of 167.8 cm and a weight of 60 kg, shown in Figure 1.

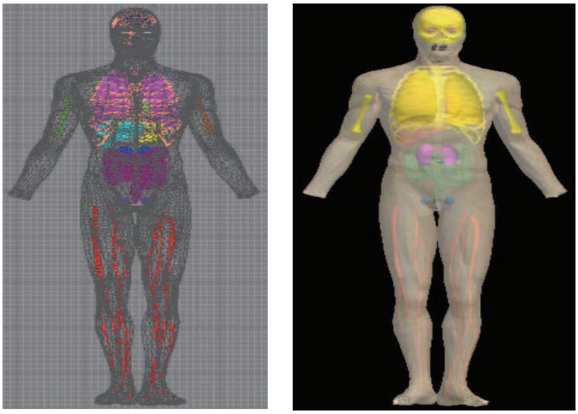

(a) (b)

Figure 1. (a) Cross-sectional line diagram and (b) solid body model of the human body .

3.3. Curve Fitting of the Electrical Parameters of the Human Body Tissue

The electrical parameters of living tissues in the electromagnetic model vary with the frequency changes of the electromagnetic field. As the irradiation source is UWB, the relationship of the changes in the electrical parameters of living tissues and those in frequencies is crucial to establish the electromagnetic model. In this study, the spline (cubic spline data interpolation) function was used to form the data interpolation and curve fitting program using Matlab 6.0. The fitting curve of relative permittivity ε_r and the conductivity σ of 12 tissues or organs between 20 MHz and 1 GHz, including brain, eye, heart, lung, stomach, intestines, liver, kidney, bone, testicle, and blood is presented in Figure 2 to Figure 13.

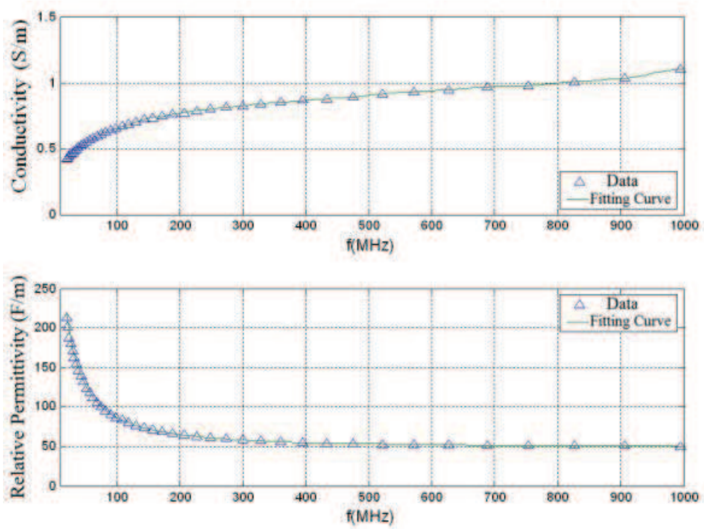

Figure 2. Variation relationship between the electrical parameters of brain tissue and frequencies.

From this curve fitting technique, the electrical parameter values of each tissue or organ at each frequency point can be extracted for the following SAR calculation of the electromagnetic model.

3.4. SAR Calculation Results

In this study, UWB is a bipolar pulse with a repetition frequency of 100 pps and width of 5 ns. Over 99% of the energy was concentrated

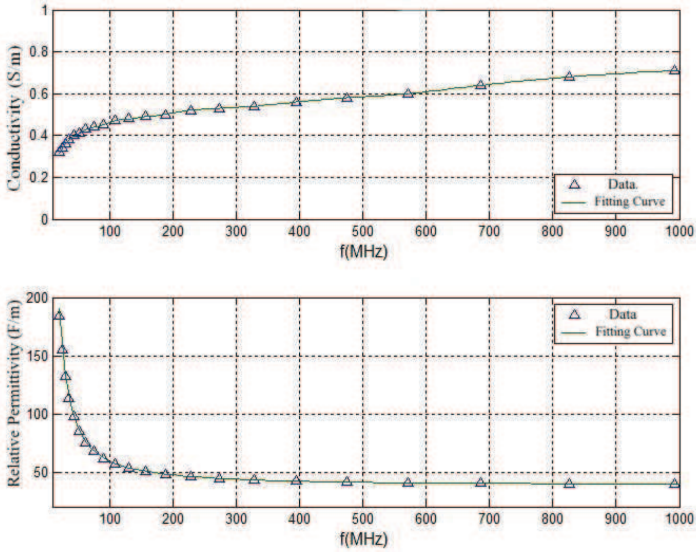

Figure 3. Variation relationship between the electrical parameters of skin tissue and frequencies

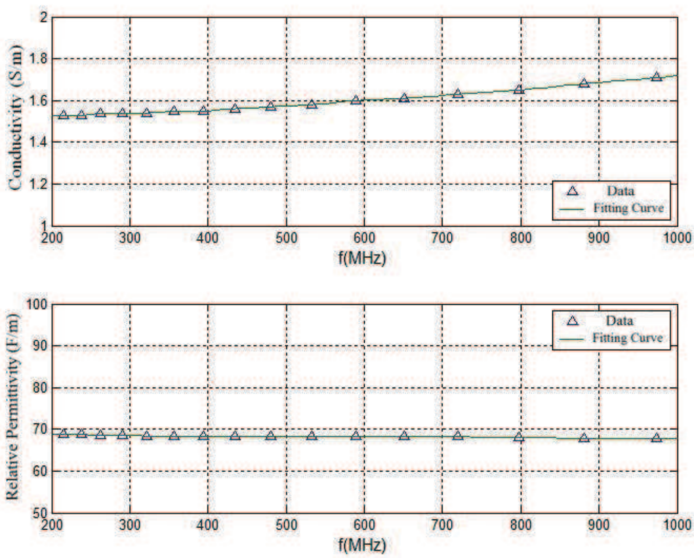

Figure 4. Variation relationship between the electrical parameters of eyeball and frequencies.

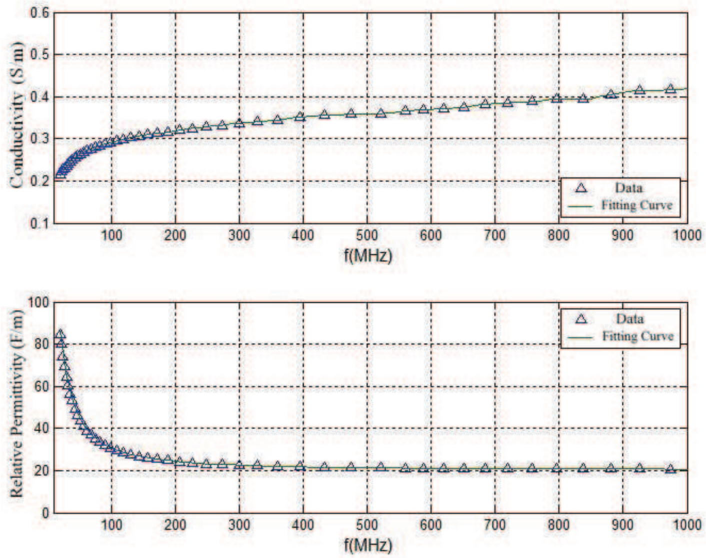

Figure 5. Variation relationship between the electrical parameters of lung and frequencies.

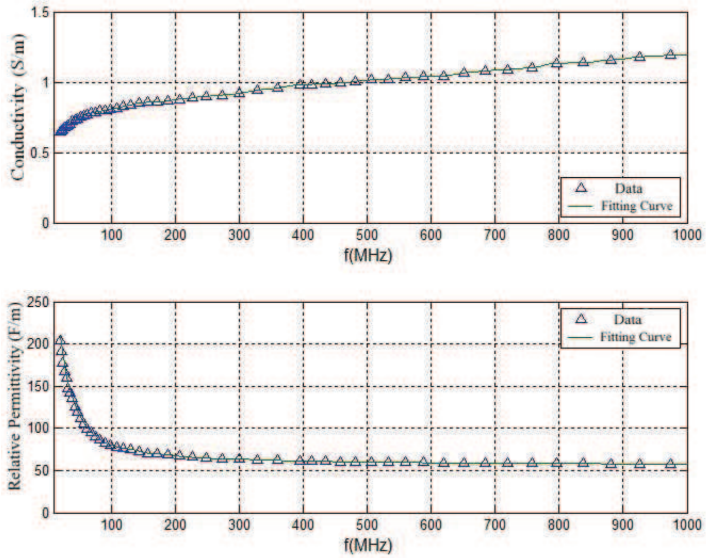

Figure 6. Variation relationship between the electrical parameters of heart and frequencies.

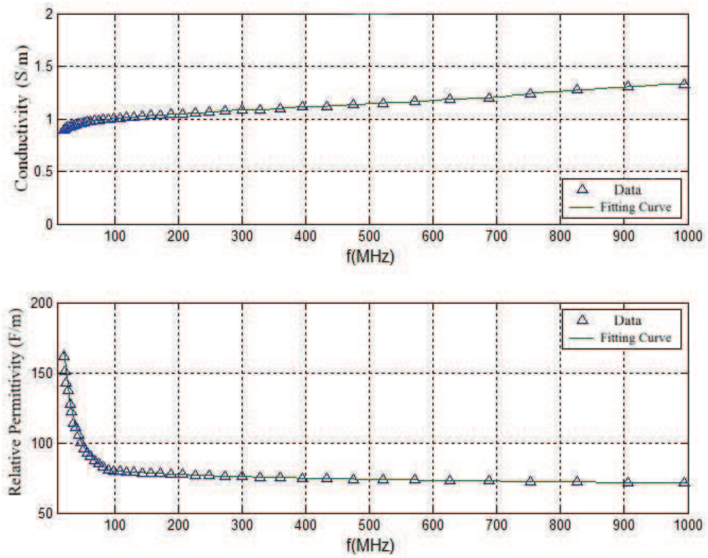

Figure 7. Variation relationship between the electrical parameters of stomach and frequencies.

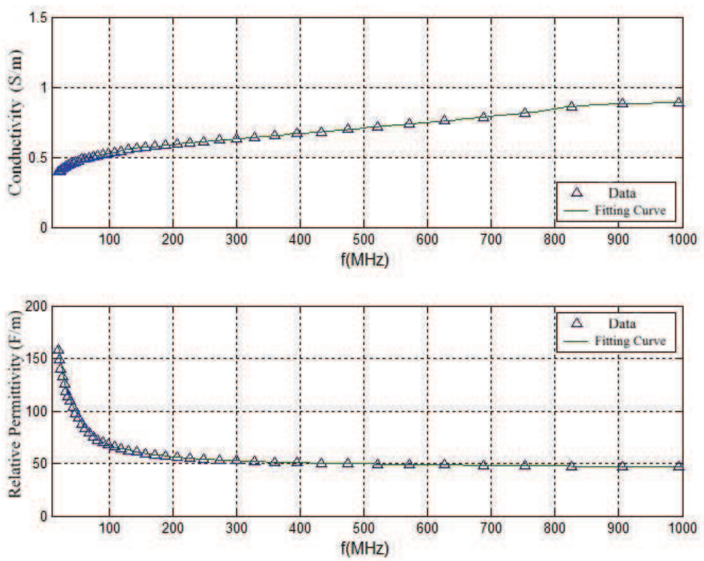

Figure 8. Variation relationship between the electrical parameters of liver and frequencies.

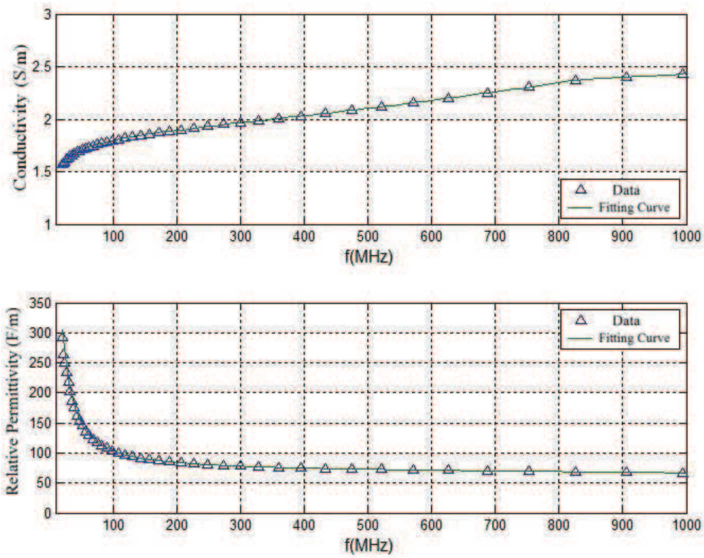

Figure 9. Variation relationship between the electrical parameters of intestine and frequencies.

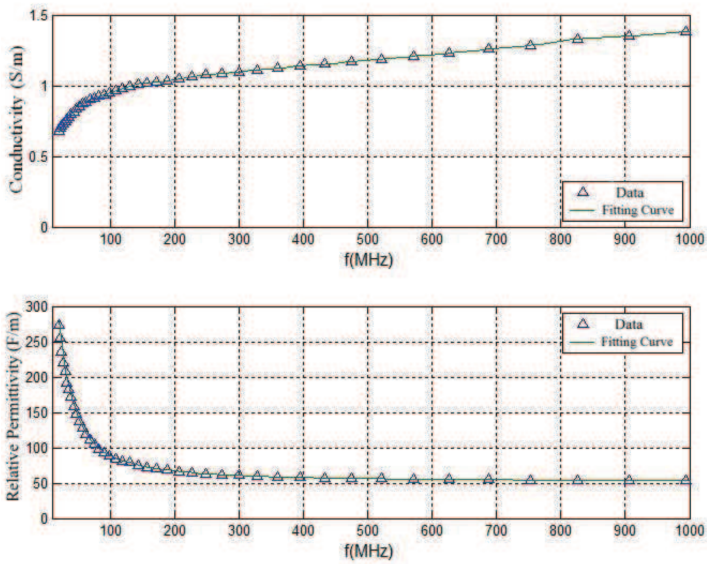

Figure 10. Variation relationship between the electrical parameters of kidney and frequencies.

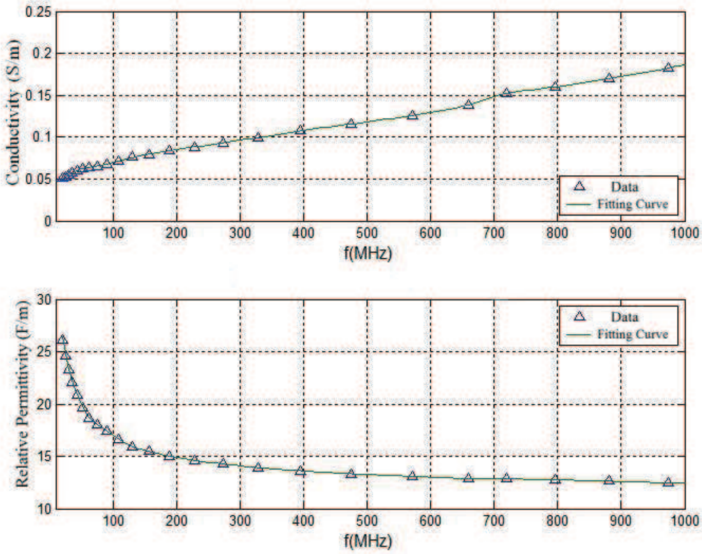

Figure 11. Variation relationship between the electrical parameters of bone and frequencies.

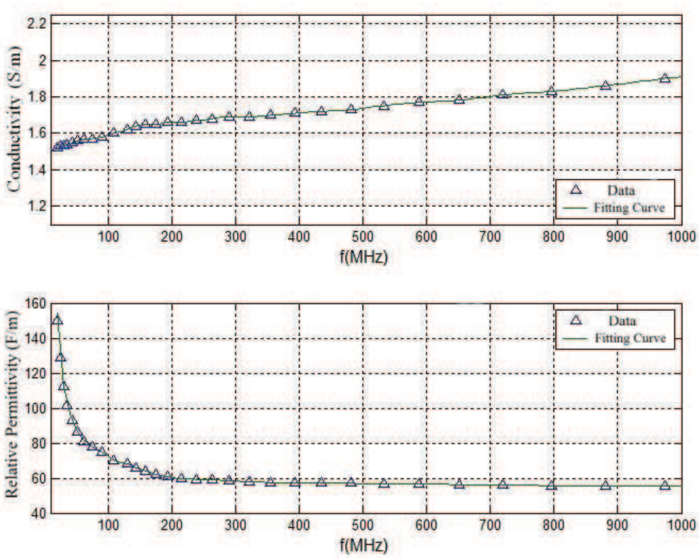

Figure 12. Variation relationship between the electrical parameters of blood and frequencies.

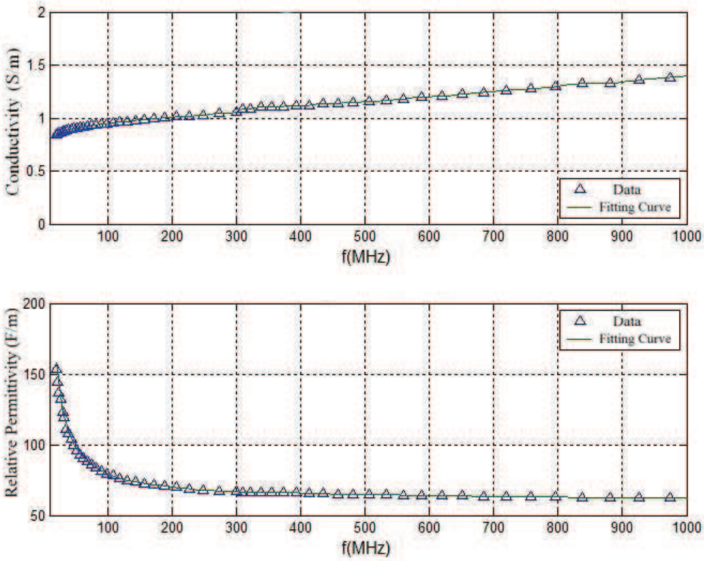

Figure 13. Variation relationship between the electrical parameters of testnis and frequencies.

between 20 MHz and 1 GHz. As the FDTD could not be directly used in solving the effect of UWB electromagnetic pulse on the objectives, this research adopted a method to make the UWB electromagnetic pulse equivalent to the accumulation effects of several time-harmonic fields that could be directly calculated with the FDTD.

The time-harmonic field frequency is 180 MHz, and the amplitude is 19.1 V/m. This time-harmonic field frequency can be used to select the calculation parameters for the SAR distribution in the male adult model. With the tissue or organ distribution in the 3-D structure of the male adult body serving as reference, medium parameters of the electromagnetic model can be identified. Furthermore, the relative dielectric constant ε_r, electrical conductivity σ, and density ρ can be determined (Table 1). Assume that the incident electromagnetic wave is a plane wave, and that the power density of free space is $P = E^2/377 = 0.097\,\mathrm{mW/m^2}$. Taking the same grid cell size along three axes of the 3-D calculation space of the Yee cell, we can obtain $\Delta x = \Delta y = \Delta z = \delta$, where $\delta = \frac{\lambda}{100} = \frac{c}{100f} = 0.017\,\mathrm{m}$, λ is the wavelength in the medium, c is the speed of light (the vacuum speed of electromagnetic waves), and f is the frequency (180 MHz). Different frequencies can generate different discrete grid sizes. The

SAR distribution of different human tissues or organs is shown in Table 1.

The SAR distribution of different human tissues or organs when $f = 40$ and 500 MHz is shown in Tables 2 and 3.

Table 1. SAR distribution of the human model under electromagnetic irradiation at 180 MHz.

Tissue or Organ	Subcutaneous Tissue	Cerebrum	Bulbus Oculi	Heart	Lungs	Stomach
ρ (kg/m^3)	1025	1038	1100	1050	330	1050
ε_r	51.2	73.6	69.1	70.6	23.6	77.9
σ (S/m)	0.47	0.74	1.50	0.80	0.31	1.04
SAR (mW/kg)	1.41	2.67	3.20	1.31	0.70	1.28
Tissue or Organ	Intestine	Liver	Kidney	Bone	Testis	Blood
ρ (kg/m^3)	1042	1030	1020	1920	1044	1008
ε_r	86.5	58.6	73.8	15.8	72.8	63.9
σ (S/m)	1.88	0.54	1.01	0.08	0.99	1.63
SAR (mW/kg)	2.15	0.65	0.34	0.26	0.32	0.90

Table 2. SAR distribution of the human model under electromagnetic irradiation at 40 MHz.

Tissue or Organ	Subcutaneous Tissue	Cerebrum	Bulbus Oculi	Heart	Lungs	Stomach
ρ (kg/m^3)	1025	1038	1100	1050	330	1050
ε_r	54.8	75.2	69.5	73.2	24.8	78.2
σ (S/m)	0.45	0.73	1.48	0.76	0.30	1.01
SAR (mW/kg)	1.41	2.67	3.20	1.31	0.70	1.28
Tissue or Organ	Intestine	Liver	Kidney	Bone	Testis	Blood
ρ (kg/m^3)	1042	1030	1020	1920	1044	1008
ε_r	91.6	63.2	76.6	16.2	74.2	66.5
σ (S/m)	1.82	0.53	1.01	0.08	0.99	1.63
SAR (mW/kg)	2.15	0.65	0.34	0.26	0.32	0.90

Table 3. SAR distribution of the human model under electromagnetic irradiation at 500 MHz.

Tissue or Organ	Subcutaneous Tissue	Cerebrum	Bulbus Oculi	Heart	Lungs	Stomach
ρ (kg/m^3)	1025	1038	1100	1050	330	1050
ε_r	51.2	73.6	69.1	70.6	23.6	77.9
σ (S/m)	0.47	0.74	1.50	0.80	0.31	1.04
SAR (mW/kg)	1.41	2.67	3.20	1.31	0.70	1.28
Tissue or Organ	Intestine	Liver	Kidney	Bone	Testis	Blood
ρ (kg/m^3)	1042	1030	1020	1920	1044	1008
ε_r	86.5	58.6	73.8	15.8	72.8	63.9
σ (S/m)	1.88	0.54	1.01	0.08	0.99	1.63
SAR (mW/kg)	2.15	0.65	0.34	0.26	0.32	0.90

4. CONCLUSION

A precise 3-D model of a Chinese adult man is built using computer-aided design software (3ds Max). Then, an electromagnetic model is established by applying the electrical parameters of various tissues and organs to the body model. The electromagnetic absorption of the electromagnetic model under the irradiation of UWB electromagnetic wave is calculated using an FDTD-based computational electromagnetic method. Then, the SAR of the ensemble average of the body model and the SAR of 12 tissues and organs are obtained. The tissues and organs used in this study, namely, subcutaneous tissue, brain, eyeball, heart, lung, stomach, intestine, liver, kidney, bone, testis, and blood, are important in the research on the bio-effects of electromagnetic pulse. By studying the SAR under electromagnetic pulse based on the body model, the following conclusions are drawn: 1. The eyeball has the highest SAR among all the human organs because it is directly exposed to electromagnetic wave and loses heat slowly, given its large water content and few blood vessels. In general, the eyeball is the organ that is most sensitive to the irradiation of electromagnetic wave. 2. The proposed model produces highly precise SAR values compared with the simple single-medium spheroid model. It can also obtain the electromagnetic field distribution inside the object model and the SAR of interior tissues and organs. 3. The FDTD method is not suitable for the research on UWB features and on the dispersion characteristics of real biosomes. The proposed method decomposes UWB to the composition of a number of continuous wave to study the absorption dose of the biosomes with dispersion characteristics under the irradiation of UWB electromagnetic pulses. The computation results thus provide a dosimetry reference for research on various subjects.

ACKNOWLEDGMENT

This work was supported by the Science Foundation of Shaanxi Province under Award Numbers 2010K13-02-01 and 2011JM4034 as well as by the Military under Award Numbers 12BJZ52 and 2011-JL2-037.

REFERENCES

1. Lu, S.-T., S. P. Mathur, Y. Akyel, and J. C. Lee, "Ultrawide-band electromagnetic pulses induced hypotension in rats," *Physiology & Behavior*, Vol. 65, 753–761, 1999.
2. Pakhomov, A. G., P. Gajsek, L. Allen, B. E. Stuck, and M. R. Murphy, "Comparison of dose dependences for bioeffects of continuous-wave and high-peak power microwave emissions using gel-suspended cell cultures," *Bioelectromagnetics*, Vol. 23, 158–167, 2002.
3. Miler, S. A., M. E. Bronson, and M. R. Murphy, "Ultrawideband radiation and pentylenetetrazol-induced convulsions in rats," *Bioelectromagnetics*, Vol. 20, 327–329, 1999.
4. Natarajan, M., Vijayalaxmi, M. Szilagyi, F. N. Roldan, and M. L. Meltz, "NF-kB DNA-bingding activity after high peak power pulsed microwave (8.2 GHz) exposure of normal human monocytes," *Bioelectromagnetics*, Vol. 23, 271–277, 2002.
5. Taflove, A. and S. C. Hagness, *Computational Electrodynamics: The Finite Diference Time-Domain Method*, Artech House, Boston, 2000.
6. Valuev, I., A. Deinega, A. Knizhnik, and B. Potapkin, "Creating numerically efficient FDTD simulations using generic C++ programming," *ICCSA 2007*, O. Gervasi and M. Gavrilova (Eds.), LNCS 4707, Part III, 213–226, 2007.
7. Gedney, S. D., "Introduction to the finite-difference time-domain (FDTD) method for electromagnetics," *Synthesis Lectures on Computational Electromagnetics*, Vol. 6, No. 1, 1–250, 2011.

8. Gan, T. H. and E. L. Tan, "Stability and dispersion analysis for three-dimensional (3-D) leapfrog ADI-FDTD method," *Progress In Electromagnetics Research M*, Vol. 23, 1–12, 2012.
9. Guo, X. M., Q. X. Guo, W. Zhao, and W. H. Yu, "Parallel FDTD simulation using numa acceleration technique," *Progress In Electromagnetics Research Letters*, Vol. 28, 1–8, 2012.
10. Dev, S. R. S., Y. Gariépy, V. Orsat, and G. S. V. Raghavan, "FDTD modeling and simulation of microwave heating of in-shell EGGS," *Progress In Electromagnetics Research M*, Vol. 13, 229–243, 2010.
11. Sabri, M. M. and J. Rashed-Mohassel, "Application of FDTD-based macromodeling for signal integrity analysis in practical PCBS," *Progress In Electromagnetics Research Letters*, Vol. 5, 45–55, 2008.
12. Yan, Y., S. Shi, and D. Ge, "Complex object modeling for FDTD method," *Journal of Xidian University*, Vol. 25, 389–392, 1998.